HCCI Engine Control by Thermal Management

J. Martinez-Frias, S.M. Aceves, D. Flowers, J.R. Smith, R. Dibble

U.S. Department of Energy

Lawrence
Livermore
National
Laboratory

May 11, 2000

DISCLAIMER

HCCI ENGINE CONTROL BY THERMAL MANAGEMENT

Joel Martinez-Frias, Salvador M. Aceves, Daniel Flowers, J. Ray Smith
Lawrence Livermore National Laboratory
7000 East Ave., L-640
Livermore, CA 94551
saceves@llnl.qov

and

Robert Dibble
Department of Mechanical Engineering
University of California
6159 Etcheverry Hall
Berkeley, CA 94720-174

ABSTRACT

This work investigates a control system for HCCI engines, where thermal energy from

exhaust gas recirculation (EGR) and compression work in the supercharger are either

recycled or rejected as needed. HCCI engine operation is analyzed with a detailed

chemical kinetics code, HCT (Hydrodynamics, Chemistry and Transport), that has been

extensively modified for application to engines. HCT is linked to an optimizer that

determines the operating conditions that result in maximum brake thermal efficiency,

while meeting the restrictions of low NO_x and peak cylinder pressure. The results show

the values of the operating conditions that yield optimum efficiency as a function of

torque and RPM. For zero torque (idle), the optimizer determines operating conditions

that result in minimum fuel consumption. The optimizer is also used for determining the

maximum torque that can be obtained within the operating restrictions of NO_x and peak

cylinder pressure. The results show that a thermally controlled HCCI engine can

successfully operate over a wide range of conditions at high efficiency and low

emissions.

INTRODUCTION

Homogeneous Charge Compression Ignition (HCCI) engines are being considered as a future alternative for diesel engines. HCCI engines have the potential for high efficiency (diesel-like, Suzuki et al., 1997), very low nitrogen oxide (NO_x) and very low particulate emissions, and low cost (because no high-pressure injection system is required). Disadvantages of HCCI engines are high hydrocarbon (HC) and carbon monoxide (CO) emissions, high peak pressures, high rates of heat release, reduced operating range, reduced power per displacement, and difficulty in starting and controlling the engine.

HCCI was identified as a distinct combustion phenomenon about 20 years ago. Initial papers (Onishi et al., 1979, and Noguchi et al., 1979) recognized the basic characteristics of HCCI that have been validated many times since then: HCCI ignition occurs at many points simultaneously, with no flame propagation. Combustion was described as very smooth, with very low cyclic variation. Noguchi et al. (1979) conducted a spectroscopic study of HCCI combustion. Many radicals were observed, and they were shown to appear in a specific sequence. In contrast, with spark-ignited (SI) combustion all radicals appear at the same time, spatially distributed through the flame front. These initial HCCI experiments were done in 2-stroke engines, with low compression ratio and very high exhaust gas recirculation (EGR).

Najt and Foster, 1989, were first to run a four-stroke engine in HCCI mode. They also analyzed the process, considering that HCCI is controlled by chemical kinetics, with negligible influence from physical effects (turbulence, mixing). Najt and Foster used a simplified chemical kinetics model to predict heat release as a function of pressure, temperature, and species concentration in the cylinder.

Recent analyses of HCCI engines have used detailed chemical kinetics codes (Lund, 1978; Kee et al., 1996) in either single zone mode (Christensen et al., 1998, Aceves et al., 1999), or multiple zone mode (Aceves et al., 2000). Single zone models assume that the combustion chamber is a well-stirred reactor with uniform temperature, pressure and composition. This model is applicable to homogeneous charge engines, where mixing is not a controlling factor. Single zone analyses can predict start of combustion with good accuracy if the conditions at the beginning of the compression stroke are known, and therefore can be used to evaluate ranges of operation for different fuels and conditions (Flowers et al., 1999). On the other hand, single zone models cannot take into account the effect of temperature gradients inside the cylinder. The assumption of uniform charge temperature inside the cylinder results in all the mass igniting at the same time when the ignition temperature is reached. Therefore, a single zone model underpredicts the burn duration, and also overpredicts peak cylinder pressure and NO_x, and is unable to predict HC and CO emissions. HC and CO emissions result from cold mass in crevices and boundary layers, which are too cold to burn to completion. A multi-zone model (Aceves et al., 2000) can take full account of temperature gradients inside the cylinder, and therefore can do a much better job at predicting peak cylinder pressure, NO_x and burn

duration, and can generate predictions for HC and CO emissions. These benefits are obtained at the cost of a much-increased time for computation compared with a single zone model.

This paper addresses the problem of controlling combustion in an HCCI engine. This is a difficult problem, due to the extreme sensitivity of HCCI combustion to temperature, pressure and composition during the compression stroke. There are many possibilities for HCCI engine control: variable compression ratio, variable valve timing, operation with multiple fuels, and thermal control. Out of these options, thermal control is inexpensive to implement and purely based on technologies familiar to manufactures and may be most acceptable if demonstrated to be satisfactory.

Considered here is a purely thermal control system for HCCI engine, where thermal energy from EGR and compression work in the supercharger are either recycled or rejected as needed. The thermal control system consists of a preheater to increase fuel-air mixture temperature, a supercharger to increase mixture density and an intercooler to decrease mixture temperature. The resulting system has five independent control parameters: equivalence ratio, fraction of EGR, intake pressure, preheater effectiveness, and intercooler effectiveness. These parameters can be tuned to meet the load demands while obtaining autoignition at the desired time and meeting the constraints of maximum pressure and NO_x emissions.

Engine control maps are determined that show the values of these five parameters to achieve the desired output torque and engine speed (rpm). The analysis uses simplified models for preheater, supercharger, and intercooler, and the engine is analyzed with a single-zone detailed chemical kinetics code (HCT).

ANALYSIS

Figure 1 shows a schematic of the thermal control system for an HCCI engine. Combustion in the HCCI engine is analyzed with a single zone HCT model. HCT has been modified to include models for all the auxiliary components considered in the system. The system is analyzed under the following set of assumptions.

- The engine operates at steady-state conditions. The problem of transitioning between operating points is not considered.

- Pressure drop and thermal losses in valves, tubes, etc., are negligible. This assumption was verified by calculating pressure losses through typical duct lengths during maximum flow conditions. The resulting pressure drops are very small.

- Heat release in the catalytic converter due to fuel oxidation is neglected. Heat transfer losses and pressure drop through the catalytic converter are also neglected.

- Pressure drop in heat exchangers is negligible. This assumption is later verified to be appropriate for this application.

- The combustion efficiency is given by the following expression:

$$\eta_c = 0.94 \qquad \text{if } \theta_{max} < 0$$

$$\eta_c = 0.94 - 0.00667\theta_{max} \qquad \text{if } \theta_{max} \geq 0 \qquad (1)$$

where η_c is the combustion efficiency and θ_{max} is the crank angle for maximum heat release ($\theta_{max}=0$ at TDC, $\theta_{max}>0$ after TDC). This expression is obtained from the experimental results of Christensen et al. (1998).

- The volumetric efficiency is assumed to vary linearly as a function of RPM, from 85% at 600 rpm to 95% at 4000 rpm, down to 90% at 5000 rpm, as reported for typical production engines (Heywood, 1988).

The characteristics of the engine and the natural gas fuel used in the analysis are given in Table 1. The dimensions of the engine correspond to the Volkswagen TDI engine, which is well known as a modern diesel engine with high efficiency and performance. The system components are described next. The geometric compression ratio selected for the analysis is 18:1.

1. HCCI Engine

The engine computations in this study were carried out using the HCT model (Hydrodynamics, Chemistry and Transport; Lund, 1978). This model has been extensively validated, having been used in a large number of investigations over the years. In particular, HCT was used in studies of engine knock and autoignition (Westbrook et al., 1988; Westbrook et al., 1991; Pitz et al., 1991). The reaction mechanism used in this work includes species through C_4 (Curran et al., 1995), and

models natural gas autoignition chemistry. The mechanism includes NO_x kinetics from the Gas Research Institute mechanism version 1.2 (Frenklach et al., 1995). The chemical kinetic reaction mechanisms used by the model for methane ignition and NO_x production have been extremely well established and are widely used. The mechanism includes 179 species and 1125 chemical reactions.

For this paper, HCT is used in single zone mode. As previously discussed, a multi-zone model can yield better predictions for engine performance than a single zone model. However, the much longer routines the multi-zone model makes it impossible to make the great number of runs required to generate an engine performance map. The single zone model can predict the conditions necessary for HCCI ignition, and it is therefore appropriate for this application. However, it is necessary to keep in mind that the single zone model overestimates peak cylinder pressure and NO_x emissions.

The performance map is form based in 7 torques at 7 engine speeds for a total of 49 operating points. In this analysis the optimizer needed an average of 100 runs of the HCT code per torque-speed point. So, 4900 times of 10 minutes HCT runs were required, for a total computational time of 820 hours.

The computational model treats the combustion chamber as a homogeneous reactor with a variable volume. The mixed temperature of the residual gases and the fresh charge is estimated by a published procedure (Heywood, 1988). The volume is changed with time using a slider-crank equation. The heat transfer submodel employed in the HCT code

simulations uses Woschni's correlation (Woschni, 1967). The cylinder wall, piston and head are all assumed to be at a uniform 430 K. Engine friction calculations are based on the method by Patton et al. (1989).

2. Preheater.

The preheater is a heat exchanger located between the exhaust gas and the intake mixture of air and fuel. Energy of the exhaust gas is used to increase the temperature of the intake ambient air. The preheater is used mainly at low power conditions or at idle, where the intake air is not heated by compression in the supercharger. Under these conditions, the intake air may be too cold to react if it is not heated. The performance of the preheater is specified by determining a value for its effectiveness, defined as:

$$\varepsilon_p = \frac{(\dot{m}c_p)_0(T_1 - T_0)}{(\dot{m}c_p)_{min}(T_{11} - T_0)} \qquad (2)$$

where subscripts 0, 1 and 11 indicate locations in Figure 1, and $(mc_p)_{min}$ is the minimum of $(mc_p)_0$ and $(mc_p)_{11}$. In this case the minimum heat capacity rate $(mc_p)_{min}$ is equal to the heat capacity rate of the intake fuel-air mixture $(mc_p)_0$. Therefore Equation (1) can be expressed as,

$$T_1 = T_{11} * \varepsilon_p + T_0 (1 - \varepsilon_p) \qquad (3)$$

Again, the pressure drop through preheater is neglected.

3. Supercharger

The supercharger is necessary to increase the engine power output. The supercharger has the additional effect of heating the engine charge, which may be necessary to obtain combustion under some conditions. Equation (3) relates conditions upstream (state 2 in Figure 1) and downstream (state 3) of the supercharger,

$$T_3 = T_2 \left(\frac{P_3}{P_2} \right)^{\frac{\gamma_2 - 1}{\gamma_2 \eta_p}} \tag{4}$$

where γ_2 is the ratio c_p/c_v in the state 2, and η_p is polytropic efficiency, assumed equal to 0.8 (Wilson, 1993).

4. Intercooler

The intercooler is necessary under some conditions to control the autoignition timing. The increase in pressure and temperature of the fuel-air mixture due to the supercharging may excessively advance heat release. Under these conditions, it is necessary to cool the mixture to obtain autoignition at the right time. The intercooler effectiveness is given by:

$$\varepsilon_i = \frac{(\dot{m}c_p)_4 (T_3 - T_4)}{(\dot{m}c_p)_{min} (T_3 - T_{i,w})} \tag{5}$$

in this case the minimum heat capacity rate $(mc_p)_{min}$ is equal to $(mc_p)_4$. Equation (4) then reduces to,

$$T_4 = T_{i,w} * \varepsilon_i + T_3 (1 - \varepsilon_i) \tag{6}$$

The analysis neglects pressure drop through the intercooler.

5. Burner

A burner is used to solve the engine startability problem, and for preheating the catalytic converter. To start the engine it is necessary to increase the fuel-air mixture inlet temperature to obtain autoignition at the desired time. The burner only needs to operate for a short period of time. Once the engine starts, hot EGR is available for continuous engine operation. The burner would use same fuel as the engine. The present paper includes only steady-state operation. Therefore, the burner is not considered in the analysis and is presented as a possibility to handle the start up problem.

SYSTEM OPTIMIZATION

For optimization of engine operating conditions, HCT is linked to SUPERCODE (Haney et al., 1995). SUPERCODE is an optimizer originally developed for the U.S. Magnetic Fusion Program for optimizing tokamak reactors and experimental designs (Galambos et al., 1995). It has subsequently been used to optimize inertial fusion devices, rail-guns, hybrid vehicles (Aceves et al., 1996) and dehumidifiers (Aceves and Smith, 1998). SUPERCODE is ideally suited for complex optimization problems with multiple decision variables and equality and inequality constraints.

For the engine optimization problem, there are five decision variables that can be adjusted to obtain the desired torque output and rpm, while maintaining satisfactory combustion and emissions. The five decision variables and their allowable ranges are:

1. Fuel-air equivalence ratio, $0.1 \leq \phi \leq 0.8$

2. Fraction of EGR, $0.05 \leq EGR \leq 0.7$

3. Preheater effectiveness (Equation 2), $0 \leq \varepsilon_p \leq 0.6$

4. Supercharger outlet pressure (Equation 3), $1 \text{ bar} \leq P_3 \leq 3 \text{ bar}$

5. Intercooler effectiveness (Equation 4), $0 \leq \varepsilon_i \leq 0.6$

The preheater and the intercooler are not used at the same time. When $\varepsilon_p > 0$, $\varepsilon_i = 0$, and when $\varepsilon_i > 0$, $\varepsilon_p = 0$. Two constraints are also introduced in the analysis. These are:

1. NO_x concentration in the exhaust is less than 100 parts per million (ppm). This guarantees ULEV (ultra low) emissions for any operating condition. Emissions for low power operation are likely to be much lower than this.

2. The peak cylinder pressure is less than 250 bar. This value is higher than the reported maximum pressure for the VW TDI engine (Neumann et al., 1992). However, the single zone model used in the analysis is known to overpredict peak cylinder pressure, so it is considered that this constraint would yield acceptable operating conditions in a real engine.

Three different optimizations are done for different operating conditions.

1. For zero torque (idle), the optimizer finds the conditions for minimum fuel consumption.

2. For any given non-zero torque, the optimizer maximizes the brake thermal efficiency of the system.

3. To determine the maximum torque, the optimizer maximizes torque with no concern for efficiency. However, the peak cylinder pressure and NO_x restrictions still have to be met.

RESULTS

The results of the analysis are shown in Figures 2 through 10. Figure 2 shows optimum brake thermal efficiency as a function of torque for a single speed of 1800 rpm. The solid line represents the optimum brake thermal efficiency when the preheater is used to condition the charge. The dotted line represents the optimum brake thermal efficiency when the intercooler is used. The figure shows that using the preheater is a better option, since it results in a higher efficiency. The intercooler is only used when the required torque cannot be reached with the preheater. Figure 2 shows that the maximum torque that can be obtained using the preheater is 118 N-m. From 118 N-m to maximum torque (140 N-m) the supercharger and intercooler operate for conditioning the charge. Figure 2 also shows that the maximum brake thermal efficiency is 40% for a torque of 124 N-m, having a very small decrease for maximum torque (39% for 140 N-m). Maximum torque is simultaneously limited by the two restrictions: NO_x is 100 ppm and maximum pressure is 250 bar.

Figure 3 through 7 show the values of the five decision variables (supercharger outlet pressure, equivalence ratio, EGR, and preheater and intercooler effectiveness, respectively) needed to achieve the desired engine output conditions (torque and rpm). These figures show full performance maps, illustrating the value of the decision variables over a broad range of engine speeds (600 to 5000 rpm).

Figures 3 through 7 show performance maps limited in the bottom by a line of zero torque (idle) and in the top by the line of maximum torque. The maximum torque is 140 N-m, and it is obtained at 1800 rpm. From this point, the maximum torque drops to 100 N-m at minimum speed (600 rpm) and to 115 N-m at maximum speed (5000 rpm).

Figure 3 shows contours of constant supercharger outlet pressure (intake pressure for the HCCI engine), as a function of rpm and torque. For very low torque it is optimum to operate the engine with atmospheric intake. Then the supercharger is used to increase the intake pressure as torque increases. The maximum supercharger outlet pressure is 2.6 bar at maximum speed (5000 rpm) and maximum torque for this speed (125 N-m).

Figure 4 shows contours of constant equivalence ratio as a function of rpm and torque. Equivalence ratio increases monotonically with torque, and in general it also increases with speed. Minimum equivalence ratio at idle is 0.25, and the maximum equivalence ratio is 0.54 for 130 N-m and 3100 rpm.

Figure 5 shows contours of constant EGR as a function of rpm and torque. For zero

torque, EGR is 0.5. EGR decreases rapidly as torque increases. At high torque, the

minimum value of EGR (0.05 corresponding to no external EGR) is reached. From this

point, EGR remains at 0.05 up to the line of maximum torque.

Figure 6 shows contours of constant preheater effectiveness as a function rpm and torque.

For idle operation, the intake temperature has to be increased to obtain satisfactory

combustion. This requires a high preheater effectiveness. From this point, the preheater

effectiveness decreases steadily. Operation of the supercharger compresses and increases

the temperature of the charge. Therefore, less preheating is required as the intake pressure

increases. For high intake pressures, the charge temperature is too high, and the preheater

is no longer needed. Instead of that, the intercooler has to be operated to achieve

satisfactory combustion.

Figure 7 shows contours of constant intercooler effectiveness as a function of rpm and

torque. The intercooler is first operated when the torque is around 90 N-m, and the

maximum intercooler effectiveness is 60% at maximum power. As previously discussed,

the intercooler and the preheater never operate simultaneously. This explains why the

lines of zero effectiveness for preheater (Figure 6) and intercooler (Figure 7) are

identical. The line of zero effectiveness indicates the transition from preheater operation

to intercooler operation.

The dimensions of the heat exchangers have been calculated by a published procedure (Kays and London, 1964). These dimensions are important, because they determine how well the system can be packaged into a vehicle. The thermal mass of the heat exchangers is also important in determining the required time for transitioning between operating points. The main characteristics of both heat exchangers (preheater and intercooler) are listed in Table 2. Heat exchangers are analyzed as cross flow heat exchangers. The preheater operates between the inlet fuel-air mixture and the exhaust gases. The intercooler is a gas-liquid heat exchanger between water from the cooling system (assumed at 373 K) and the intake mixture. The preheater total volume is 1.6 liters and the intercooler total volume is 3.0 liters. Pressure drops are small in all cases (less than 190 Pa), validating the original assumption of neglecting pressure drops in heat exchangers.

Figure 8 shows contours of constant peak cylinder pressure as a function of rpm and torque. Peak cylinder pressure for low torque (less than 40 N-m) is almost constant at 50 bar. Between 40 and 110 N-m the peak cylinder pressure increases about linearly (from 50 to 150 bar) as the torque increases. Then, the peak cylinder pressure increases rapidly as torque increases further. At maximum torque, the peak cylinder pressure reaches its higher bound (250 bar).

Figure 9 shows contours of constant NO_x emissions in parts per million (ppm) as a function of rpm and torque. NO_x emissions are near zero for zero torque. As the torque increases, NO_x emissions increase rapidly, due to the higher equivalence ratio required

for achieving the desired torque (Figure 4). At high torque, NO_x emissions approach their higher bound (100 ppm), and there is a broad area near the maximum torque where NO_x emissions are practically at their limit. This indicates that relaxing the constraint on maximum NO_x could increase the maximum power. For a vehicular application, the engine would not be designed with a hard limit on NOx emissions, as considered here. Instead, the vehicle would have to meet the relevant emissions standards under a given driving cycle. Therefore, it may be possible to considerably enhance the maximum torque calculated in this analysis, depending on the particular vehicle application.

Figure 10 shows lines of constant brake thermal efficiency as a function of torque and rpm. The figure shows solid lines representing constant efficiency for the engine in HCCI mode. The figure also shows dotted lines, which represent the efficiency of the TDI engine in diesel mode (Converted from Neumann et al., 1992). The figure shows that the engine working in HCCI mode is more efficient for low torque at any engine speed than the engine working in diesel mode. This result is very significant, considering that the VW TDI engine is well recognized as a small, high efficiency diesel engine. The engine has a higher efficiency in HCCI mode because of the faster combustion obtained with HCCI combustion, and the need to delay combustion to reduce NO_x emissions in the diesel engine. However, the maximum torque is higher for the TDI engine in diesel mode (180 N-m, compared to 140 N-m). Maximum torque is therefore reduced by 22% due to HCCI operation. Maximum power is reduced by 12% (from 67 kW to 59 kW) due to HCCI operation. As previously discussed, maximum HCCI engine power can be increasing by relaxing the NO_x constraint (or possibly by lowering the compression ratio)

in vehicular applications. This change would have to be evaluated according to the particular characteristics of the vehicle and it is therefore not considered here.

CONCLUSIONS

This paper presents a methodology for controlling an HCCI engine, where thermal energy from exhaust gas recirculation (EGR) and compression work in the supercharger are either recycled or rejected as needed. HCCI engine operation is analyzed with a detailed chemical kinetics code, which is linked to an optimizer that determines the operating conditions that result in maximum brake thermal efficiency, while meeting the restrictions of low NO_x and peak cylinder pressure. Five decision variables are used in the optimization: equivalence ratio, exhaust gas recirculation (EGR), intake pressure, preheater effectiveness and intercooler effectiveness. The results show the values of the operating conditions that yield optimum efficiency as a function of torque and engine speed. The results show that the HCCI engine can be successfully operated over a wide range of conditions, with a brake thermal efficiency significantly higher than obtained in diesel mode. NO_x emissions are restricted to 100 ppm, and are much lower at low power. The major disadvantage of HCCI operation is the reduced maximum engine torque, which is 22% lower than the engine can obtain in diesel mode. The HCCI engine is more efficient than the TDI in diesel mode for the same torque operating points. Changing other parameters, such as decreasing compression ratio or relaxing NO_x limit, could allow for increased maximum torque.

REFERENCES

Aceves, S.M., Smith, J. R, L.J. Perkins, S.W. Haney, and D.L. Flowers, "Optimization of a CNG Series Hybrid Concept Vehicle," SAE Paper 960234, SAE International Congress and Exposition, Detroit, February 1996.

Aceves, S.M., and Smith, J. R., 1998, "A Desiccant Dehumidifier for Electric Vehicle Heating," ASME Journal of Energy Resources Technology, Vol. 120, No. 2, pp. 131-136.

Aceves, S.M., Smith, J. R., Westbrook, C, and Pitz, W., 1999, "Compression Ratio Effect on Methane HCCI Combustion," ASME Journal of Gas Turbines and Power, Vol. 121, pp. 569-574, 1999.

Aceves, S. M., Flowers, D. L., Westbrook, C. K., Smith, J. R., and Dibble, R. W., 2000, "A Multizone Simulation of HCCI Combustion and Emissions," SAE paper 2000-01-0327.

Christensen, M., Johansson, B., Amneus, P., and Mauss, F., 1998, "Supercharged Homogeneous Charge Compression Ignition," SAE Paper 980787.

Curran, H. J., Gaffuri, P., Pitz, W. J., Westbrook, C. K., and Leppard, W. R., 1995, "Autoignition Chemistry of the Hexane Isomers: An Experimental and Kinetic Modeling Study," SAE paper 952406.

Flowers, D. L., Aceves, S. M., Westbrook, C. K., Smith, J.R., and Dibble, R. W., 1999, "Sensitivity of Natural Gas HCCI Combustion to Fuel and Operating Parameters Using Detailed Kinetic Modeling," In AES-Vol. 39, "Proceedings of the ASME Advanced Energy Systems Division - 1999," Edited by S.M. Aceves, S. Garimella and R. Peterson, pp. 465-473.

Frenklach, M.,Wang, H., Goldenberg, M., Smith G. P., Golden, D. M., Bowman, C. T., Hanson, R. K., Gardiner, W. C.,and Lissianski, V., 1995, "GRI-Mech - An Optimized Detailed Chemical Reaction Mechanism for Methane Combustion", GRI Topical Report No. GRI-95/0058.

Galambos, J.D., Perkins, L.J., Haney, S.W., and Mandrekas, J., 1995, "Commercial Tokamak Reactor Potential with Advanced Tokamak Operation," Nuclear Fusion, Vol. 35, p. 551.

Haney, S.W., Barr, W.L., Crotinger, J.A., Perkins, L.J., Solomon, C.J., Chaniotakis, E.A., Freidberg, J.P., Wei, J., Galambos, J.D., and Mandrekas, J., 1995, "A SUPERCODE for System Analysis of Tokamak Experiments and Reactors," Fusion Technology, Vol. 21, p. 1749.

Heywood, J. B., 1988, Internal Combustion Engine Fundamentals, McGraw-Hill, New York, NY.

Kays, W.M., and London, A.L., 1964, Compact Heat Exchangers, McGraw-Hill, New York, NY.

Kee, R.J., Rupley, F.M., Meeks, E., and Miller, J.A., 1996, "CHEMKIN III: A Fortran Chemical Kinetics Package for the Analysis of Gas-Phase Chemical and Plasma Kinetics," Sandia National Laboratories Report SAND96-8216, Livermore, CA, May.

Lund, C. M., 1978 "HCT - A General Computer Program for Calculating Time-Dependent Phenomena Involving One-Dimensional Hydrodynamics, Transport, and Detailed Chemical Kinetics," Lawrence Livermore National Laboratory report UCRL-52504.

Najt, P. M. and Foster, D. E., 1983, "Compression-Ignited Homogeneous Charge Combustion," SAE paper 830264.

Neumann, K.H., Kuhlmeyer, M., and Pohle, J., 1992, "The New 1.9 L TDI Diesel Engine with Low Fuel Consumption and Low Emission from Volkswagen and Audi," SIA Paper No. 92038.

Noguchi, M., Tanaka, Y., Tanaka, T., and Takeuchi, Y., 1979, "A Study on Gasoline Engine Combustion by Observation of Intermediate Reactive Products During Combustion," SAE paper 790840.

Onishi, S., Jo, S. H., Shoda, K., Jo, P. D., and Kato, S., 1979, "Active Thermo-Atmosphere Combustion (ATAC) - A New Combustion Process for Internal Combustion Engines," SAE paper 790501.

Patton, K. J., Nitschke, R. G., and Heywood, J. B., 1989, "Development and Evaluation of a Friction Model for Spark-Ignition Engines," SAE paper 890836.

Pitz, W. J., Westbrook, C. K., and Leppard, W. R., 1991, "Autoignition Chemistry of C4 Olefins Under Motored Engine Conditions: A Comparison of Experimental and Modeling Results," SAE paper 912315.

Suzuki, H., Koike, N., Ishii, H., and Odaka, M., 1997, "Exhaust Purification of Diesel Engines by Homogeneous Charge with Compression Ignition Part 1: Experimental Investigation of Combustion and Exhaust Emission Behavior Under Pre-Mixed Homogeneous Charge Compression Ignition Method," SAE paper 970313.

Westbrook, C. K., Warnatz, J., and Pitz, W. J., 1988, "A Detailed Chemical Kinetic Reaction Mechanism for the Oxidation of iso-Octane and n-Heptane over an Extended

Temperature Range and its Application to Analysis of Engine Knock," Twenty-Second Symposium (International) on Combustion, p. 893, The Combustion Institute, Pittsburgh.

Westbrook, C. K., Pitz, W. J., and Leppard, W. R., 1991, "The Autoignition Chemistry of Paraffinic Fuels and Pro-Knock and Anti-Knock Additives: A Detailed Chemical Kinetic Study," SAE paper 912314.

Wilson, D. G., 1993, The Design of High-Efficiency Turbomachinery and Gas Turbines, The MIT Press, Cambridge, Massachusetts.

Woschni, G., 1967, "Universally Applicable Equation for the Instantaneous Heat Transfer Coefficient in the Internal Combustion Engine," SAE Paper 670931

Table 1. Main characteristics of the Volkswagen TDI 4-cylinder engine used for the HCCI experiments and composition of the natural gas fuel.

Engine geometric properties	
Displaced volume	1900 cm^3
Bore	79.5 mm
Stroke	95.5 mm
Connecting rod length	145 mm
Geometric compression ratio	18:1
Natural gas composition, volume %	
Methane	91.1
Ethane	4.7
Propane	1.7
n-Butane	1.4
Nitrogen	0.6
Carbon dioxide	0.5

Table 2. Main characteristics of heat exchangers (preheater and intercooler).

Parameter	Preheater	Intercooler
Type	Cross flow	Cross flow
Fluids:		
Fluid 1	Mixture of Air and fuel	Mixture of Air and fuel and EGR
Fluid 2	Exhaust gases	Cooling water
Dimensions:		
Along flow direction of fluid 1, m	0.11	0.18
Along flow direction of fuel 2, m	0.13	0.13
Perpendicular to flow directions, m	0.11	0.13
Volume, liters	1.6	3.0
Mass, kg	0.26	0.37
Maximum effectiveness	0.6	0.6
Maximum pressure drop, fluid 1, Pa	16	190
Maximum pressure drop, fluid 2, Pa	80	70
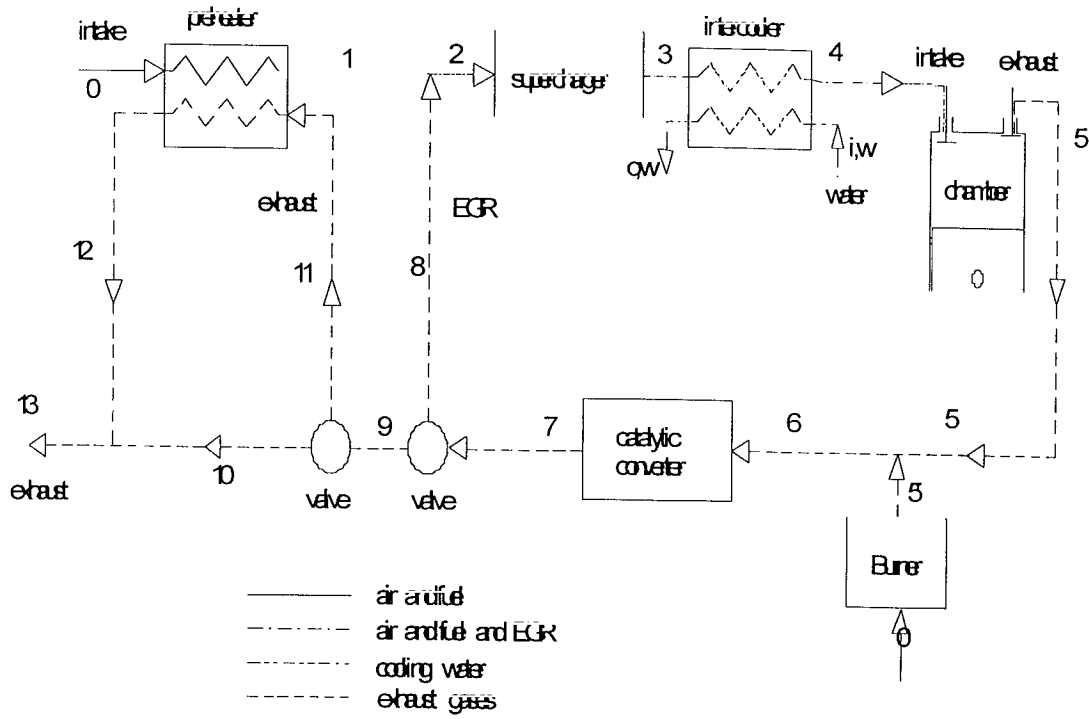
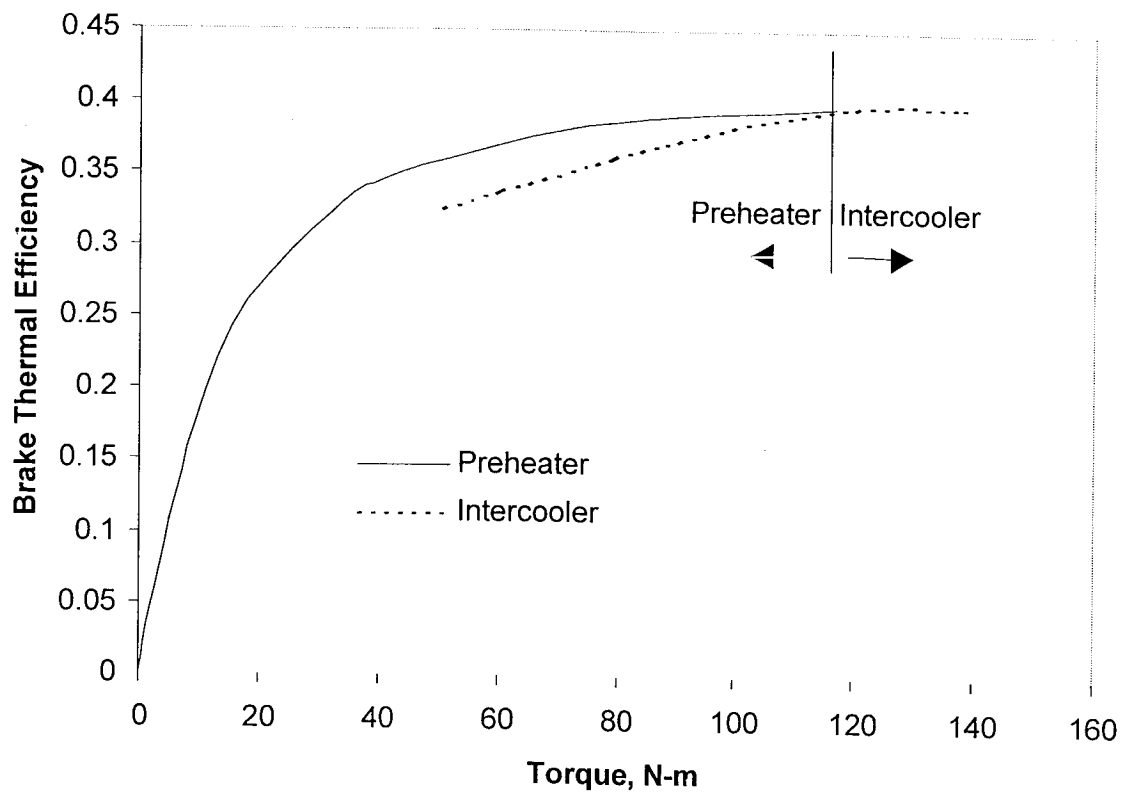Figure 1. Schematic of the thermal control system for the HCCI engine.

Figure 2. Optimum brake thermal efficiency as a function of torque, for 1800 rpm. The solid line shows the efficiency of the HCCI engine operating with the preheater. The dotted line shows the efficiency of the HCCI engine with the intercooler.
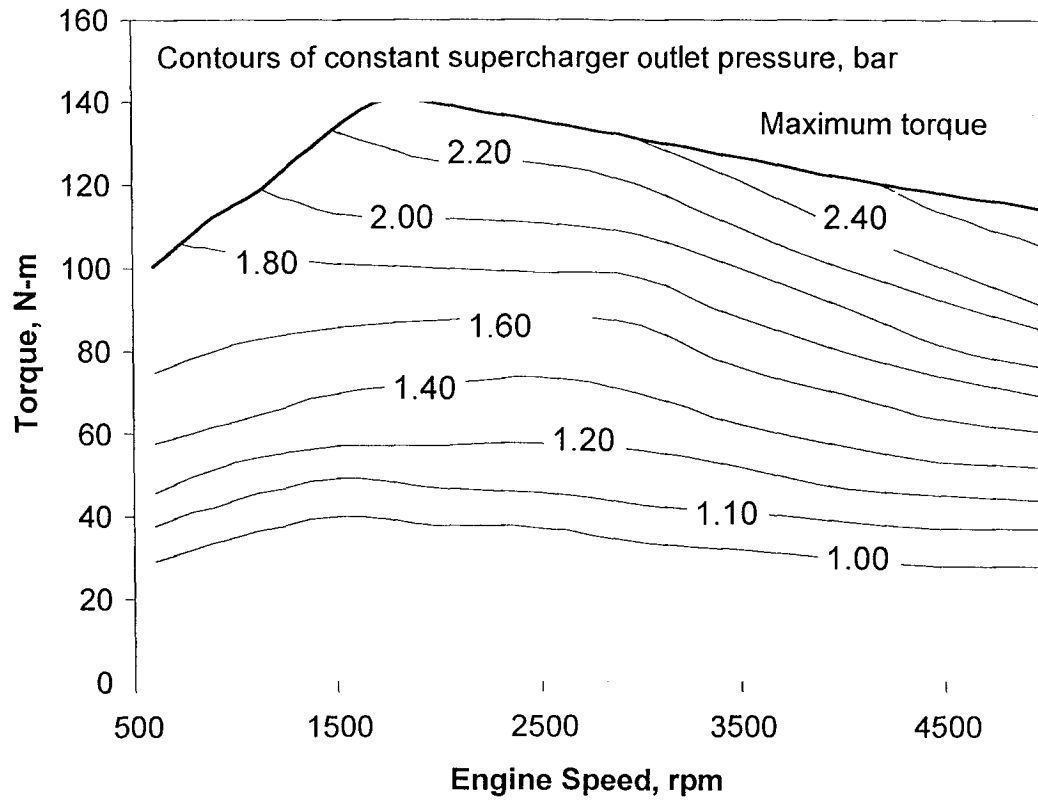
Figure 3. Contours of constant supercharger outlet pressure in bar as a function of rpm and torque. The figure also shows the line of maximum engine torque.
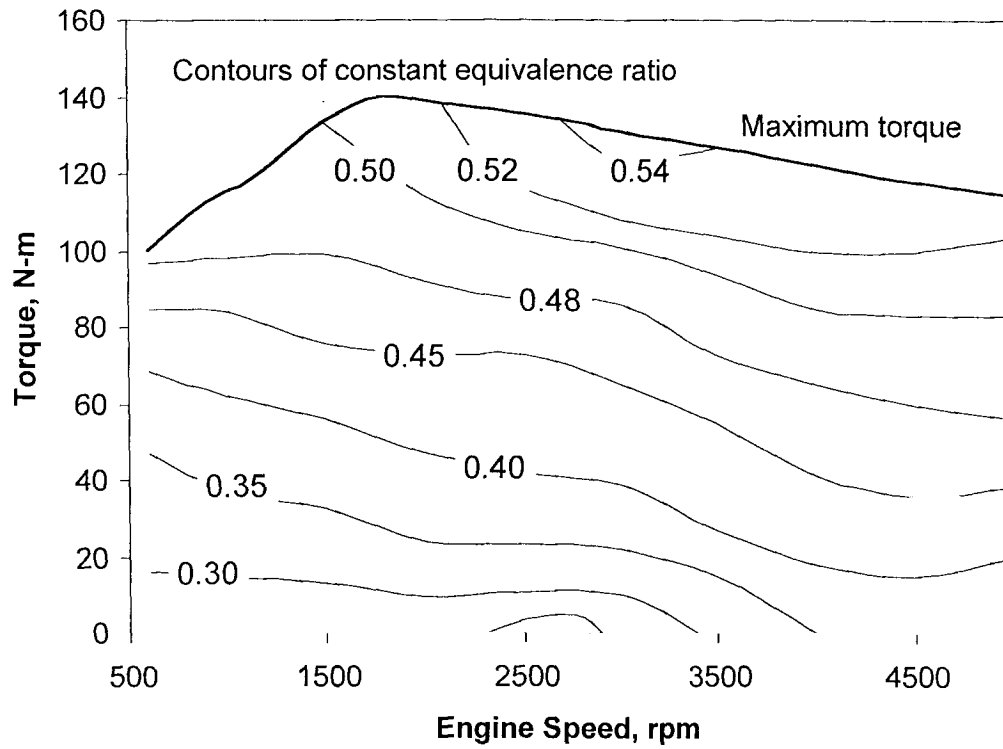
Figure 4. Contours of constant equivalence ratio as a function of rpm and torque. The figure also shows the line of maximum engine torque.
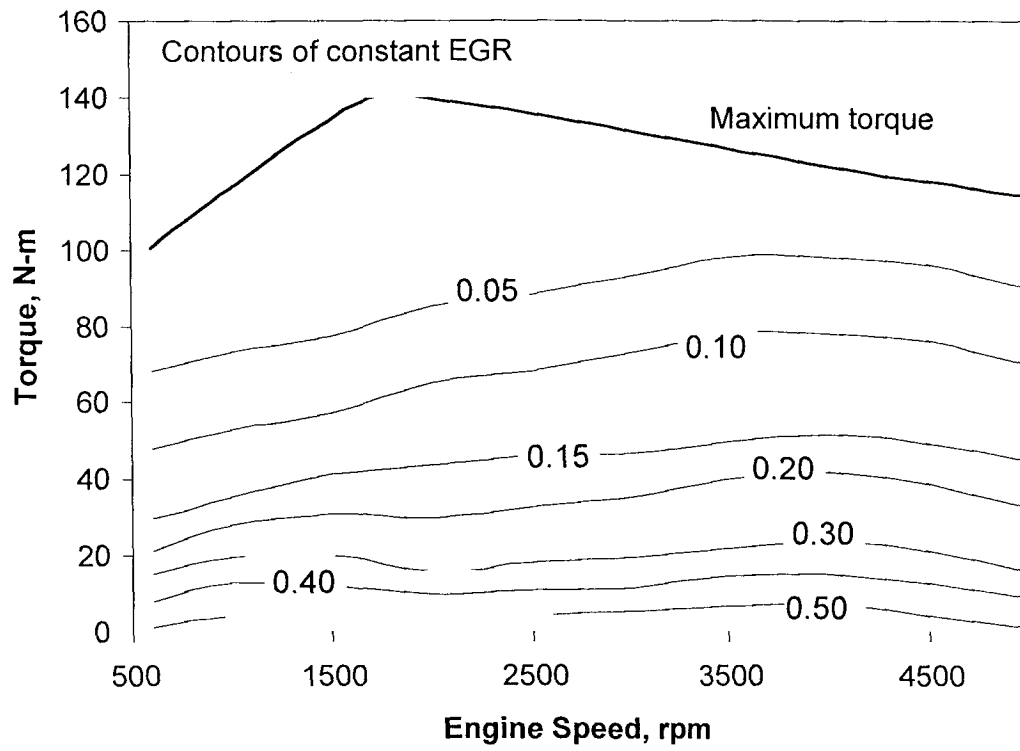
Figure 5. Contours of constant EGR as a function of rpm and torque. The figure also shows the line of maximum engine torque.
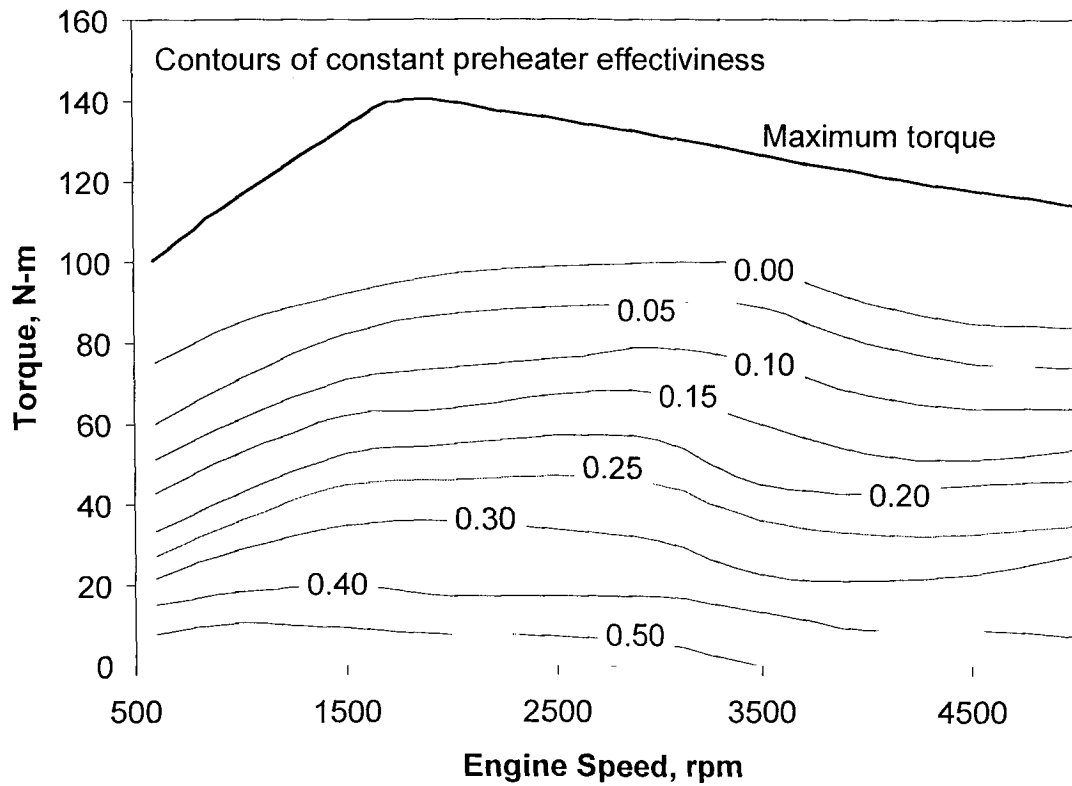
Figure 6. Contours of constant preheater effectiveness as a function of rpm and torque. The figure also shows the line of maximum engine torque.
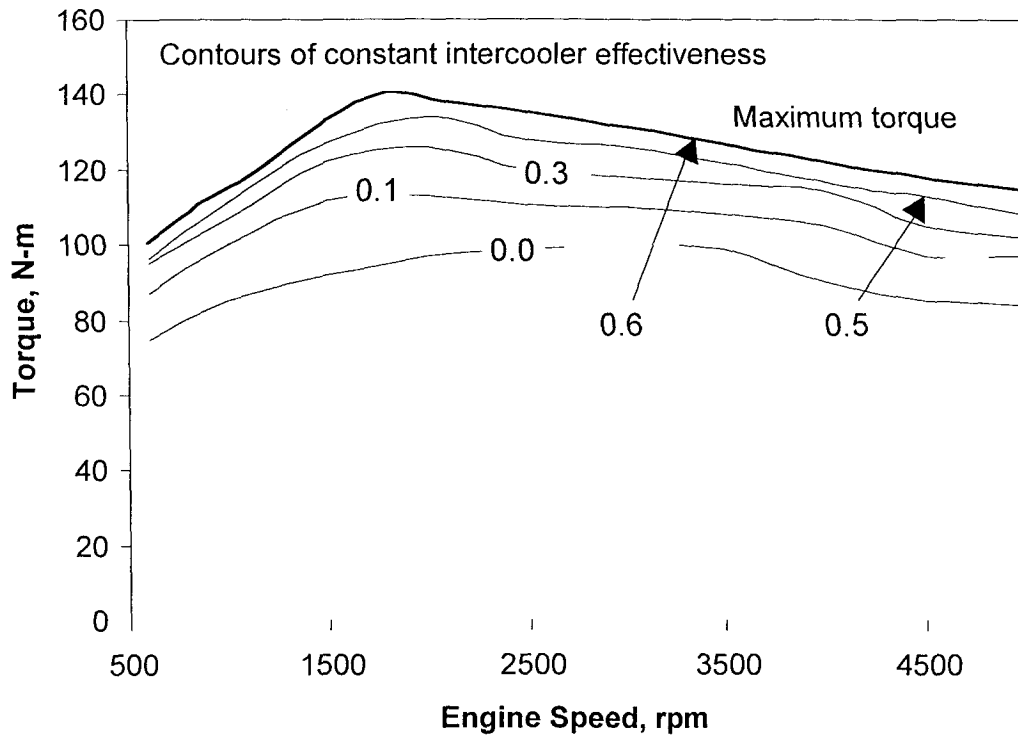
Figure 7. Contours of constant intercooler effectiveness as a function of rpm and torque. The figure also shows the line of maximum engine torque.
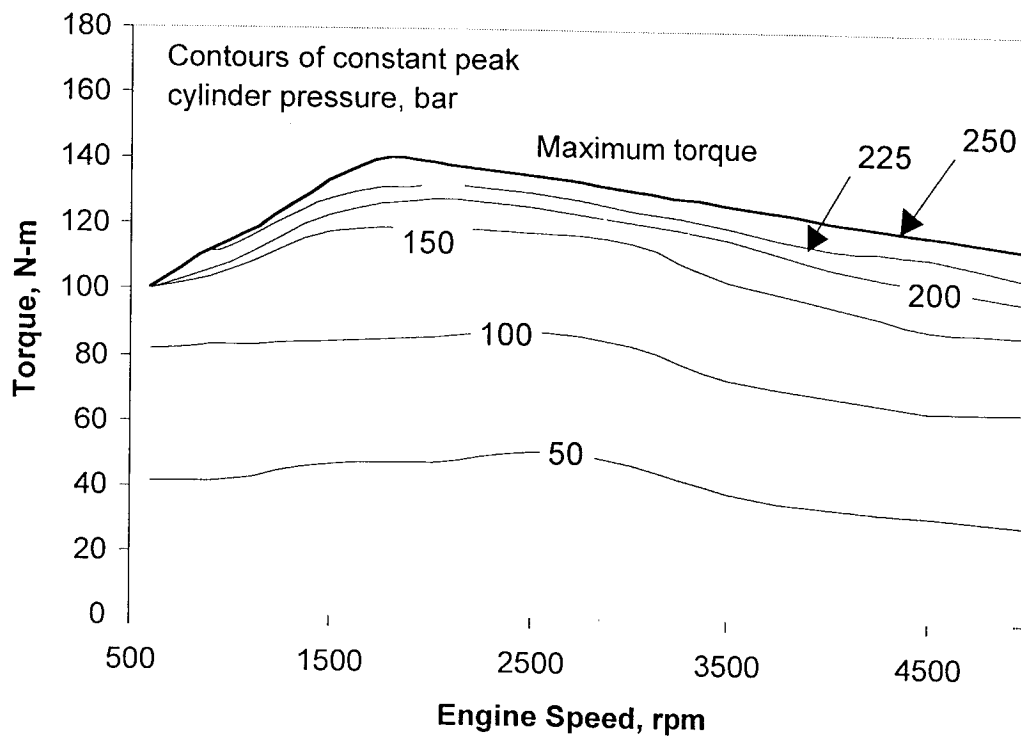
Figure 8. Contours of constant peak cylinder pressure in bar as a function of rpm and torque. The figure also shows the line of maximum engine torque.
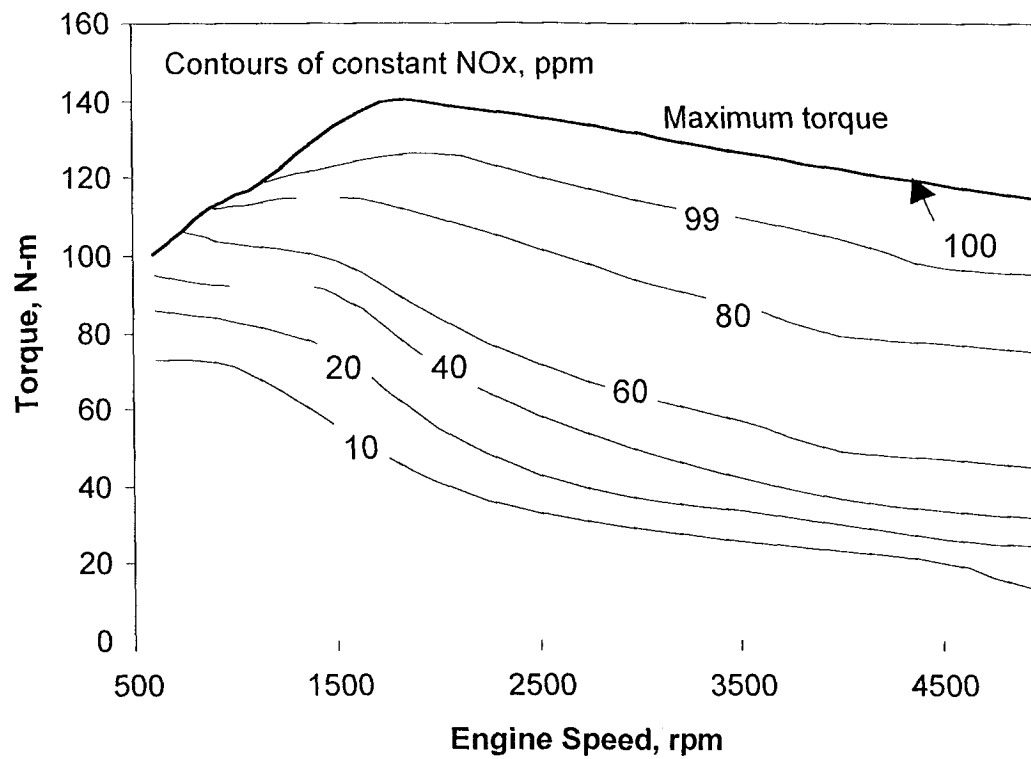
Figure 9. Contours of constant NO_x concentration in the exhaust gas as a function of rpm and torque. The figure also shows the line of maximum engine torque.
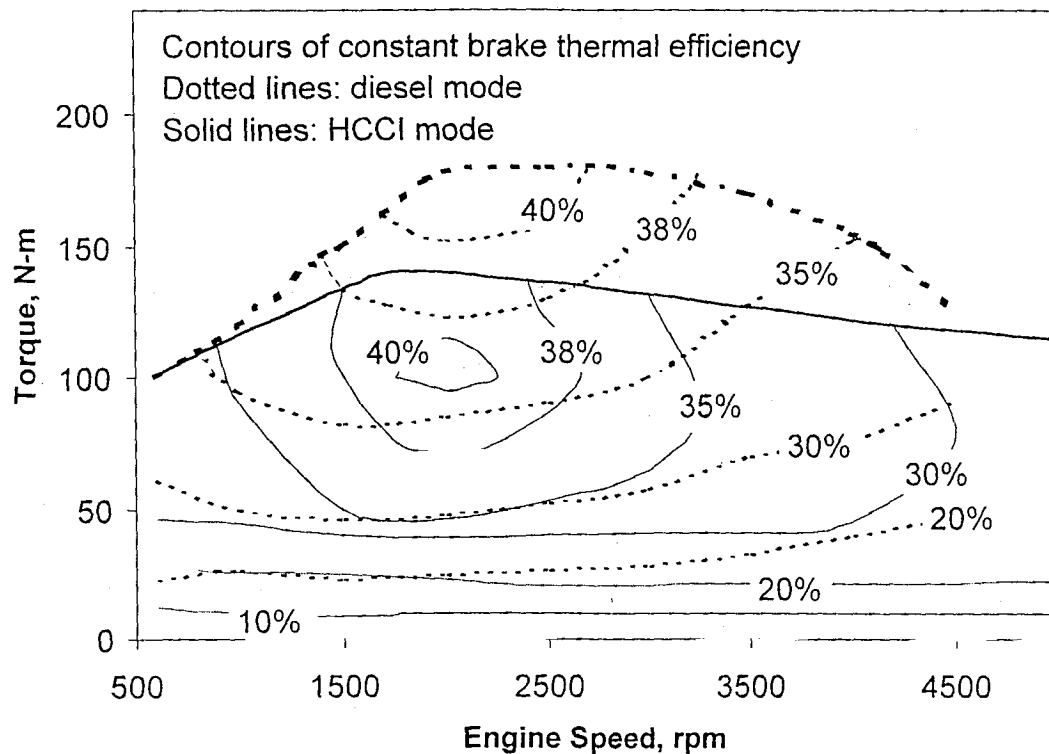
Figure 10. Performance map for the Volkswagen TDI 4-cylinder engine, showing contours of constant brake thermal efficiency. Dotted lines: diesel mode. Solid lines: HCCI mode. Lines of maximum torque are also shown for the diesel and HCCI mode as thicker lines.